Nanoformulated CPMSN biomaterial regulates proinflammatory cytokines to heal wounds and kills drug-resistant bacteria

Chandran Murugan[1], Manickam Rajkumar[1], Nagarajan Kanipandian[2], Ramasundaram Thangaraj[1], Karuppaiya Vimala[1] and Soundarapandian Kannan[1,*]

[1]Department of Zoology, School of Life Sciences, Periyar University, Salem 636 011, India
[2]Department of Hepato-Biliary Pancreatic Surgery, Henan Provincial People's Hospital, Zhengzhou, Henan Province, People's Republic of China

Chitosan (CS) is one of the most abundant biopolymers present on the wings of arthropod members like insects, prawns, etc. It has potential biomedical value in developing drugs and drug delivery systems. Such a biomedically valuable polymer was combined with mesoporous silica nanoparticles (MSNs) to form chitosan-poly (acrylic acid) coated mesoporous silica nanoparicle (CPMSN) material along with poly acrylic acid (PAA) as co-polymer. The selected polymers perfectly interact with the drugs namely topotecan and quercertin after decorating the materials with arginine-glycine-aspartic (RGD) peptide. The formulated CPMSN biomaterial was analysed biologically and chemically for its stability, biocompatibility and sustained release of drugs to heal wounds. In the present study, the efficacy of the formulated biomaterial has been well proven by *in vitro* and *in vivo* models. The present finding suggests that the drug-loaded CPMSN biomaterial significantly induces re-epithelialization process by regulating immune cells at the wound sites. The Western blot analysis revealed the activation of proinflammatory genes like *NF-kB*, *TNF*, *IL-1*, *MMP-1*, *MMP-2* and *COX2* that accounts for enhanced wound-healing cascade activation. The present study also observed antibacterial activity of the formulated biomaterial against selected bacterial species. Thus we can conclude that the CPMSN biomaterial not only possesses wound-healing properties, but also behaves as an antibacterial agent.

Keywords: Biocompatibility, chitosan, mesoporous silica nanoparticles, wound-healing.

INTENSIVE research has been undertaken in recent years to evaluate the impact of biomaterials on pathophysiology of both chronic and acute wounds on the skin[1]. Among various biomaterials, the natural or synthetic polymeric scaffolds have been widely used to prepare the wound dressing materials loaded with phytotherapeutic compounds that are biocompatible and easily degradable, and mimic the extracellular matrix of the skin[2,3]. The quality of the biomaterial is dependent on its porosity, mechanical strength and biomolecular dynamics that enhance the tissue re-development with beneficial microenvironment for wound healing[4,5]. In the present study, a biomaterial has been selected accordingly as a suitable wound dressing material to not only heal wounds but also control bacterial infections. Biopolymers like chitosan-based dressings have been studied in the context of drug delivery[6], rather than wound healing using cell lines and animal models[7]. The combination of biopolymer and synthetic polymers illustrates good biocompatibility and wound-healing properties equated with commonly used biomaterials and also has a low toxicity profile. Hence, in the present study we selected a polysaccharide, chitosan (CS) and poly acrylic acid (PAA) as the synthetic polymer to form a biomaterial to endorse collagen deposition within *in vivo* animal model. Furthermore, the selected mesoporous silica nanoparticles (MSNPs) show good structural support for cell attachment and migration, accelerating wound healing and delivering drugs with antimicrobial properties. We used topotecan (TPT) and quercetin (QT) as drugs to inhibit bacterial growth and accelerate the anti-inflammatory response during wound healing. TPT is derived from semisynthetic process of a quinoline derivative called camptothecin. This alkaloid was extracted from the bark of *Camptotheca acuminate*, which is a common tree in Asian countries. Interestingly, recent study reported that TPT has several biological applications which include cytotoxicity, DNA damage at S-phase in cell cycle, inactivation of topoisomerase I with anticancer properties[8]. A recent survey reveals that this alkaloid is limited by low stability and solubility, and unpredictable drug–drug interactions. Hence, in the present study, the stability of TPT was improved by encapsulating the compound using CS and PAA copolymers. Furthermore, the biological activity of TPT was enhanced by incorporating another phytodrug, viz. QT while formulating the chitosan-poly (acrylic acid) coated mesoporous

*For correspondence. (e-mail: skperiyaruniv@gmail.com)

silica nanoparicle (CPMSN) biomaterial[9]. QT is a colouring flavonoid present in all kinds of leafy vegetables, fruits, spices, etc.[10,11]. Thus, the present study is mainly focused on determining the synergistic effects of selected drugs and their delivery using polymeric moieties to cure skin wounds.

Materials and methods

Preparation of MSNs

We prepared MSN by following the standard protocol of Murugan et al.[9]. In a typical reaction, 0.1 g CTAB, 200 ml double distilled water and 1 ml sodium hydroxide (2 mM) solution were gently mixed using magnetic stirrer and kept at 80°C for 120 min. Later, 0.5 ml of TEOS was added dropwise into the reaction mixture and persistently maintained at 80°C for another 6 h. The white colour precipitate was collected after centrifugation at 10,000 rpm for 10 min. Around 2 ml HCl (0.1%) and 20 ml of methanol were added to the reactants to remove the unwanted materials and then the solution was heated at 80°C overnight under stirring condition at 230 rpm in a magnetic stirrer. The samples were then centrifuged and the final product collected as pellet. The pellet rinsed three times with ethanol, and finally dried overnight in a vacuum chamber at 60°C for 12 h. Then, MSN (0.1 g) was dissolved in 20 ml of anhydrous ethanol and heated to 80°C for 5 min. APS (1 ml) was added to the solution to functionalize MSN with the amino groups. The reaction mixture was refluxed for 24 h, and cooled to room temperature followed by centrifugation, washed three times with ethanol and H_2O, and dried overnight in vacuum at 45°C for 12 h to give MSN-NH_2 as a white powder.

Drug loading efficiency of TPT

Topotecan was loaded onto MSN–NH_2; 6 ml of MSN-NH_2 dispersion (1 mg/ml) was added with 2 ml aqueous solution of TPT (2 mg/ml) and the mixture was gently shaken using a rotator for 12 h at room temperature. The nanoparticles (TPT-MSN-NH_2) were obtained through centrifugation at 10,000 rpm and carefully rinsed three times with ethanol to remove the unbound TPT.

Synthesis of PAA-CS-coated TPT-MSN-NH_2

The TPT-MSN-NH_2 was dispersed (20 mg) in a 15 ml mixture of DMF and H_2O containing 0.15 mg of PAA (molecular weight, $M_w = 18,000$) and 0.35 g of CS, and the mixture was stirred at 50°C for 6 h. The resultant product was centrifuged, washed several times with deionized water to remove non-conjugated PAA-CS and dried overnight in vacuum at 45°C.

Loading of QT and grafting of cRGD on TPT-MSN-NH_2-PAA-CS

QT was suspended (25 mg) in 50 ml of aqueous solution containing 0.2 g of TPT-loaded MSN-NH_2-PAA-CS. The product was stirred at 45°C for 24 h followed by washing with double distilled water several times to remove unloaded QT. Next, 300 mg of 1-ethyl3-dimethylaminopropyl) carbodiimide (EDC) and 250 mg of N-hydroxysuccinimide (NHS) were added and further stirred at room temperature for 24 h. Subsequently, to this solution 0.01 mg of cRGD peptide was added and incubated for 2 h at room temperature to obtain CPMSNs. The adsorption measurements of the original solution and supernatant were recorded[9].

Cell culture and cytotoxicity study in vitro

The cytotoxic effects of CPMSNs were determined using a quantitative MTT assay. The NIH-3T3 fibroblast cells were grown in DMEM medium containing 10% foetal bovine serum and 10 units ml^{-1} penicillin/streptomycin at 37°C in a 5% CO_2 humidified atmosphere. Cells were seeded in a 24-well plate at a concentration of 40,000 cells/well for 24 h. The CPMSNs (30 µl) were added into the trans-well chamber. The cells cultured in DMEM were set as control. After incubation for 24 h, the trans-well chamber and medium were removed and replaced with 50 µl of MTT solution (1 mg ml^{-1} in PBS), and the cells were incubated for another 4 h. Finally, the MTT solution was removed, and 100 µl of DMSO was added per well to dissolve the crystals completely. The absorbance of each well at 570 nm was measured using a microplate reader (Multiskan FC Thermo Fisher, USA).

Histological study of wound contraction

Skin samples taken at the 7th, 14th and 21st day, and cut in small pieces. All samples were fixed in formaldehyde, paraffin-embedded, and 4 µm-thick sections were stained with hematoxylin-eosin (H&E) and Sirius Red. At days 7, 14 and 21, the upper contraction surface was observed on each corner of the wound. Skin thickness was determined at days 14 and 21 by evaluating the contraction surface at three different points, starting from the middle of the wound. The sectioned in stained slide was analysed at 10× magnification.

Expression levels of cytokines in CPMSN-treated wounds

Wounded skin biopsy material was collected from the donors (7, 14 and 21 days post-wound). Skin samples were subjected to biochemical analysis. The excised skin tissue (100 mg) was homogenized in 1 ml of 0.1 M PBS (pH = 7.4) using a glass homogenizer. The skin homogenates

were centrifuged at 10,000 rpm for 10 min at 4°C and the collected supernatants were stored at –80°C until further analysis. The homogenates were estimated for *COX-2*, *MMP-1*, *IL-4* and *TNF* contents, and prostaglandin-E2, thromboxane and leukotriens levels were measured in the culture medium using commercial ELISA kits following the manufacturer's protocol. The absorbance was noted at a particular wavelength (450 nm) specified time intervals to study the effect of CPMSN treatment compared to control groups on the wound-healing events.

Excision wound creation on mice skin and macroscopic examination

The wound-healing potential of the developed CPMSNs was evaluated using a Swiss albino mice model. The mice were anaesthetized using an intra-peritoneal injection of a mixture of xylazine and ketamine (90 and 5 mg/kg body weight respectively). The dorsal surface of mice skin was shaved and sterilized with 5% povidone/iodine solution. Circular full thickness cutaneous wound of diameter 8 mm was created around the breast regions on the dorsal surface of the mice using biopsy punch. The animals were then categorized randomly into two experimental groups (four mice/group). The wounds were treated topically with each of the CPMSN formulations daily (50 mg/day/wound) over a period of 21 days. The amount of CPMSN used was sufficient to cover the wound-bed completely. The wound site of each animal was photographed and wound diameter was measured at these time points using a vernier calliper to calculate wound closure area (%) according to the following formula

$$\text{Wound closure (\%)} = \frac{\left(\begin{array}{c}\text{Initial area of wound} - \\ \text{The } n\text{th day area of wound}\end{array}\right)}{\text{Initial area of wound}} \times 100.$$

Western blot analysis

At 21 days, the wounds were removed, fragmented and homogenized with Tris buffer (50 mM/l, pH 6.8) containing the protease inhibitor phenylmethylsulphonyl fluoride (PMSF) (10 mg/ml). The samples were placed in an ultrasonic bath (3×15 s) and centrifuged at 4°C. Total protein (μg/ml) present in the supernatant of each sample was measured by the Bradford method[12], and total protein was diluted in a solution containing 1% SDS, 2% 2-mercaptanol, and 10% glycerol, and placed in boiling water for 5 min. Separation and packaging gels containing 10% and 4% polyacrylamide respectively, and molecular weight standards from 6.9 to 200 kDa (Mark12 Unstained Standard) were used. Also, β-actin was used as a loading control. After separation by electrophoresis in SDS–PAGE, the proteins were transferred to a nitrocellulose membrane and blocked with Tris buffer solution containing 0.2% Tween-20 (TBST, pH 7.5), and 10% milk protein for 1 h. The membrane was incubated overnight with rabbit monoclonal collagen-I, collagen-III and TGF-β (1 : 250) antibody (Santa Cruz Biotechnology, Santa Cruz, CA), and washed with TBST. Nitrocellulose membrane was revealed using a secondary antibody F(ab′) 2 fragment of rabbit anti-mouse IgG (Santa Cruz Biotechnology) conjugated to HRP (1 : 1000) for 1 h. The blot was incubated in a chemiluminescence solution (Novex Chemiluminescent Substrates, Invitrogen) at room temperature, and autoradiographed with a ChemiDoc XRS system (Bio-Rad). Protein levels were analysed by densitometry (Image J 1.47 software).

Cell migration assay

NIH-3T3 cells were seeded in a tissue culture 6-well plate at an initial density of 2.4×10^5 cells/cm^2 overnight. A micropipette tip was used to create a wound in the monolayer by scraping. Next the cells were treated with CPMSN in 5% FBS DMEM. Wounded areas were photographed at time zero. After 7, 14 and 24 h of incubation, photographs were taken from the same areas as those recorded at time zero. Experiments were performed at least three times in quadruplicate. The migration rate of the cells was calculated using the following formula

$$R_M = \frac{W_i - W_f}{t},$$

where R_M is the rate of cell migration (nm/h), W_i the initial wound width (nm), W_f the final wound width (nm) and t is the duration of migration (h).

Antibacterial activity of CPMSN nanomaterials

The bacterial organisms MDR-*Escherichia coli* and MRSA-*Staphylococcus aureus* used in this study were collected and characterized at the Department of Microbiology, Periyar University, Salem. They were clinical wound isolates from patients in Salem, identified and maintained on a nutrient agar plate at 4°C at the Department of Microbiology, Periyar University until further use. Prior to use, the organisms were sub-cultured on sterile nutrient agar plate, incubated aerobically at 37°C for 24 h. Colonies of each organism were homogenized in sterile phosphate buffered saline (PBS) and the turbidity adjusted to correspond to 0.5 McFarland's turbidity standard (equivalent to 1×10^8 CFU/ml). The standardized broth cultures were set aside at 4°C until further use.

Statistical analysis

The Statistical Software 8.0 (Stat Soft, Inc. 1984–2007) was used for statistical analysis to validate our data. Here, the ± values are mean of standard deviation (SD).
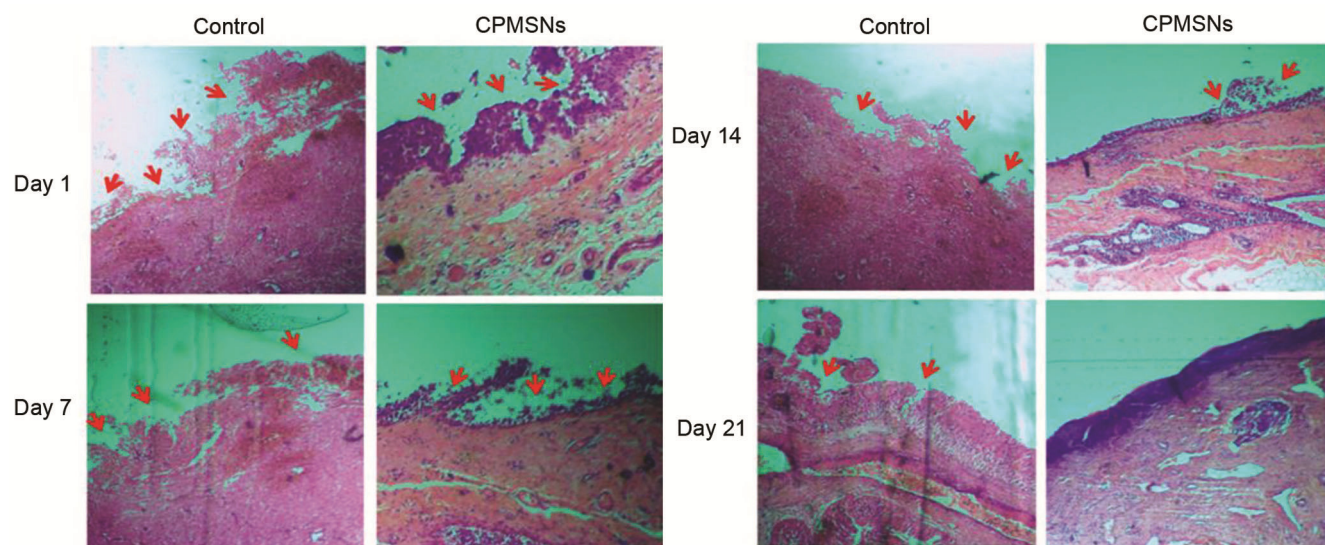
Figure 1. Bright field photomicrographs of hematoxylin and eosin staining of wounded skin tissue sections of Swiss albino mice showing changes in wound-healing events at day 1, day 7, day 14 and day 21 after wounding. The red arrows indicate re-epithelialization of the wounds on day 21 post-operatively ($n = 4$ mice per group), and once complete wound closure was noted. On day 21, there was complete re-epithelialization in the chitosan-poly (acrylic acid) (PAA) coated mesoporous silica biomaterial treated wounds. Scale bar: 50 µm (magnification 40×).

Results

Re-epithelialization in CPMSN-treated wounds

The effect of formulated CPMSN material on wounded skin was assessed. The histological observations using H&E staining revealed the modifications in wound curative efficacy like dermal restoration and epithelial regeneration (Figure 1). The healing rate was observed to be faster in wounds treated with CPMSNs after 14 days when compared to control. This reflects that CPMSNs could play a greater role in would healing as they carry dual phyto-drugs, namely TPT and QT. Furthermore, restoration of the epidermis was also noticed in the treated group which was appreciable when compared to control. The reason for decreased inflammation rate with wound dressing CPMSN biomaterial might be the existence of a large number of carboxylate moieties of PAA. After 21 days of treatment with CPMSNs, the structural integrity of the newly formed tissue mimicked natural skin with a slight scar in the wounded area. Furthermore, biopsy samples were stained with toluidine blue to explore the well-stratified epidermis, basal, spinous, granular and cornified layers with perfect vascularization at the dermal–subcutaneous interface. The chemical reactions between polymers and drugs are appreciable due to the presence of CS, PAA, QT and cRGD peptide in CPMSN biomaterial that could have fastened the tissue repair process by converting fibroblasts into myofibroblasts. We observed that the collagen fibrils scattered in an irregular fashion in the CPMSN-treated group. The entire event may be accompanied by thin granulated tissue that covers the thin epithelium with a large epithelial gap. In addi-

tion, CPMSN has been to promote rapid epithelialization due to its tendency to absorb water in nano-structural pores of the biomaterial used in the present study. In the control skin samples, tissue organization has not been re-established at a faster rate compared to the treated group owing to form disorganized and irregular structure of the dermis.

Wound closure effects of CPMSNs

Figure 2 depicts the wound closure effects for control and CPMSN-treated groups. Thus effects revealed a significant level of difference between both groups. In case of the CPMSN-treated group, wound closure activity was reported to have greater degree of wound closure than the control. On the other hand, CS and PAA present in CPMSN behave as an extracellular matrix and may provide moist and tissue micro-environment to the exuding wounds.

Expression of cytokines in CPMSN-treated wounds

Figure 3 provides an assessment of wound healing effects of CPMSNs. The cutaneous incision wound healing was evaluated using the *in vivo* animal model against the formulated CPMSN material as tissue glue or scaffolds. Normally, the wound-healing process could be divided into four overlapping but well-defined phases: hemostasis, inflammation, proliferation, and remodelling and scar formation. The perfect wound-healing agent should have the ability to induce wound closure and hemostasis. Further, this treatment improves the minimal wound-healing
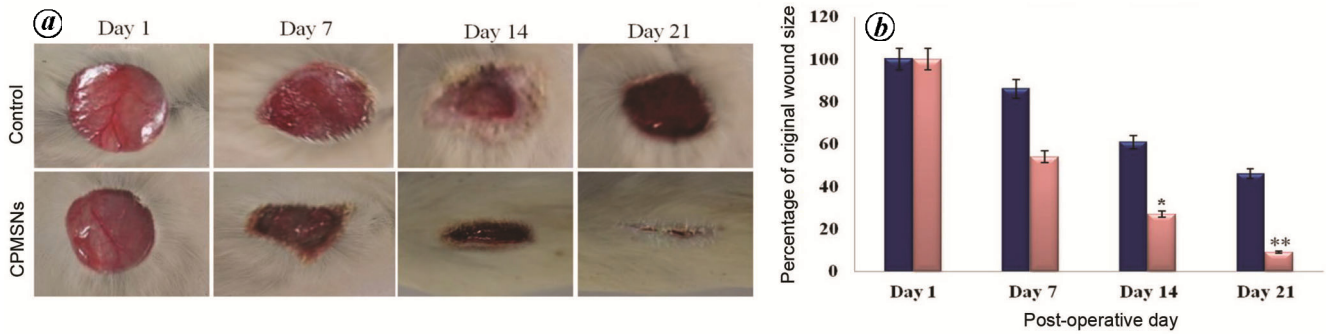
Figure 2. *a*, Wounds during post-operative treatments. *b*, Mean percentage wound closure in heterozygous mouse wounds with or without CPMSNs treatment at different time intervals, viz. day 1, day 7, day 14 and day 21. Comparison of wound-healing effects between two groups; the CPMSN wounds were significantly more closed on day 21 compared to control group ($P < 0.001$). Error bars denote standard error of the mean.
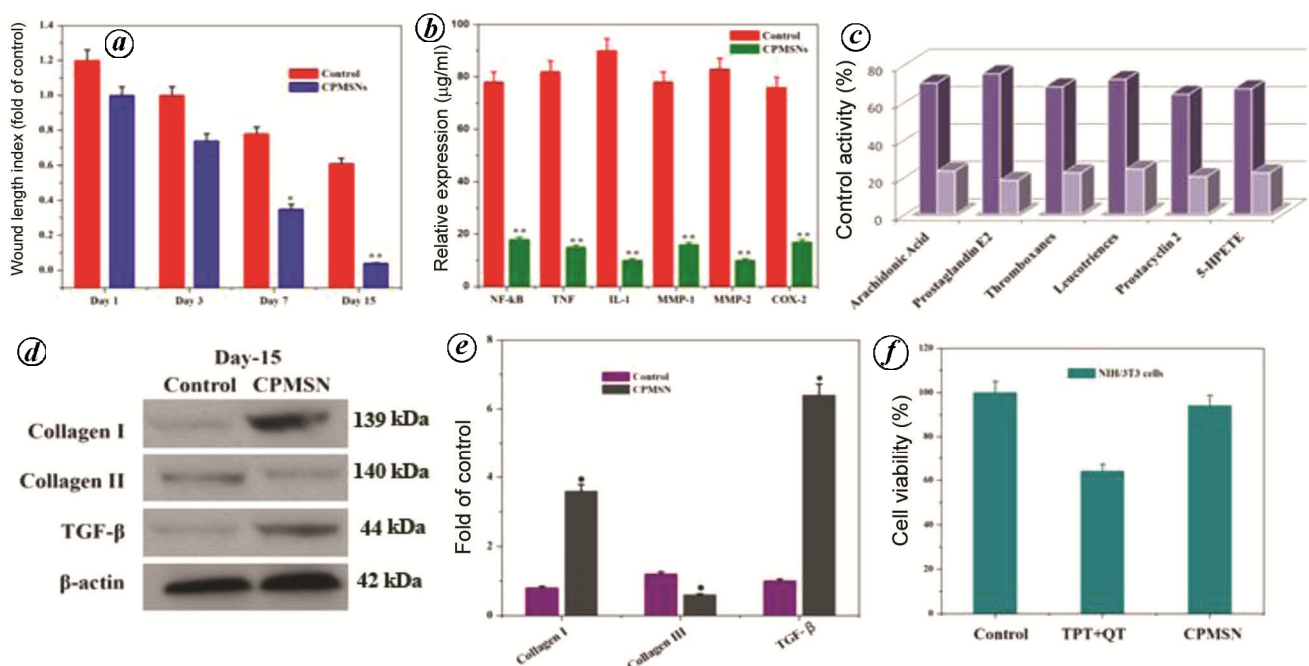

Figure 3. *a*, Comparison of percentage of wound closure efficacy of control and CPMSN-treated groups. *b*, The impact of inflammatory gene expression profile of *NF-κB*, *TNF*, *IL-1*, *MMP-1*, *MMP-2* and *COX-2* proteins in mice belonging to control and CPMSN-treated groups. *c*, *In vitro* 3D cell-culture assay for anti-inflammatory response of CPMSN in treated cells. *d*, Western blot analysis of expression profiles of collagen II, collagen I and TGF-*β* at day 21. *e*, Relative expression levels of target proteins in control and CPMSN-treated cells. *f*, Cell viability of NIH-3T3 cells treated with saline, TPT + QT and CPMSNs. Statistical data were used to compare the days of treatment between CPMSN and control groups (*$P < 0.05$). The results are expressed as mean ± standard deviation. Values are means of three independent experiments.

duration and minimizes scar formation. The percentage of CPMSNs is directly proportional to the level of tissue reconstruction or replacement of injured or disrupted tissue, and restores the mechanical strength, anatomical structure and function of repaired skin. Furthermore, the expression of pro-inflammatory genes like *NF-kB*, *TNF*, *IL-1*, *MMP-1*, *MMP-2* and *COX-2*, were noticed during wound healing process. It also acts as an effector for fibroblasts and keratinocytes multiplication to enhance the epithelialization process. In CPMSN biomaterial-treated groups at day 21, the proinflammatory genes, viz. *NF-kB*, *TNF*, *IL-1*, *MMP-1*, *MMP-2* and *COX-2* were found to be downregu-

lated when compared to control. Thus, the reduction in inflammatory proteins could be attributed to anti-inflammatory response of TPT + QT present in CPMSNs.

The study was extended to analyse the levels of eicosanoids such as prostaglandin-E2, thromboxane and leukotrienes. At the end of the treatment (day 21), TGF-*β*, collagen I, and collagen II proteins are significantly down regulated (*$P < 0.05$*). During the healing process, TGF-*β* is released from the platelets and serves as the driving force for cellular differentiation and chemotaxis of immune and inflammatory cells in the wounded region. Furthermore, TGF-*β* is essential during the last phase of

the healing process, where it converts collagen-III into collagen-I which accounts for stimulation of keratinocyte proliferation, thus supporting wound epithelialization. The Western blot indicates an increased level of collagen-I and TGF-β after 21 days of CPMSN treatment. It shows that CPMSN treatment enhances the TGF-level in wounded mice at a later stage. The cytotoxicity of CPMSN had significantly decreased compared to free drugs (TPT + QT) and control. The fibroblast cells incubated with CPMSN exhibited non-toxic effect compared to free drugs, revealing the biocompatible nature of CPMSN and improved therapeutic activity.

Cell migration assay

The induction of cell motility in NIH-3T3 cells by CPMSN treatment was evaluated by migration assay (Figure 4 a). Representative photomicrographs clearly indicated that CPMSN treatment exhibited a highly migratory potential, but in the control reduced migration potential was observed. Statistical analysis revealed a significantly increased number of migrating cells when CPMSN was present in the culture medium. As an independent measure of NIH-3T3 cell motility and studies on long-term effects of CPMSN, we performed trans-well migration assays over a period of 72 h. Similar to scratch assays, the migratory capacity of untreated cells had not changed. In both control and treated cells, CPMSNs were found to influence significant attenuation of cell migration and wound-healing rate (Figure 4 b and c). The
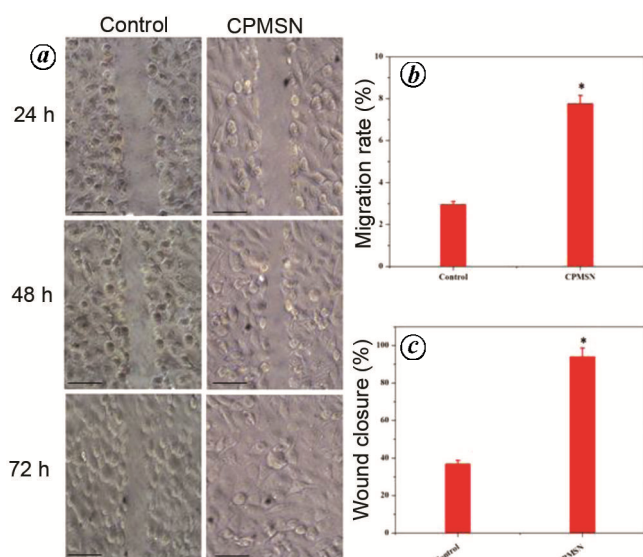

Figure 4. Effect of CPMSN on NIH-3T3 cell migration. *a*, Cell migration of NIH-3T3 cells incubated in FBS-free DMEM containing 10 µl/ml of saline and CPMSN for 24, 48 and 72 h. Scale bar: 50 µm. Determination of (*b*) migration rate and (*c*) wound closure rate in control and CPMSN-treated groups. Standard error bars represent three independent experiments and each experiment was done in triplicate (*$P < 0.05$; magnification 20×).

present findings indicate that CPMSN-mediated treatment have functional consequences in association with cell motility in the wound areas.

Antibacterial activity of CPMSN nanomaterials

To evaluate the antibacterial properties of CPMSN, the test was carried out by serial dilution method to determine the minimal inhibitory concentration (MIC) values (Figure 5). The effect of CPMSN was tested against some wound-infecting microbes such as *S. aureus* (Figure 5 a) and *E. coli* (Figure 5 b). The obtained results revealed that CPMSN significantly decreased bacterial load in the treated groups, suggesting that the extract had *in vivo* antibacterial effect against the tested microorganisms which are involved in wound contamination. The CPMSNs exhibited bacteriostatic activity against the organisms at different concentrations (25, 50, 75 and 100 µl), suggesting that these nanoparticles were bacteriostatic at lower concentrations but bactericidal at higher concentrations. The wound site during treatment with CPMSN showed significant increase in the rate of wound contraction and wound re-epithelialization is a reflection of good antibacterial potential of CPMSN, as revealed in the *in vivo* and *in vitro* antibacterial assay. The presence of QT and CS with CPMSN could be attributed to its good antioxidant property that might have promoted its antimicrobial activity. The increased concentration of CPMSN has effective antibacterial activity against Gram-positive and Gram-negative bacteria (Figure 5 c). In this context, CPMSN appears as a promising source to develop novel antibacterial agents notably to fight multi-drug resistant bacteria implicated in skin infections.

Discussion

The largest organ of our body is the skin. It is composed of the epidermis and dermis with a complex nervous system and good blood supply. Such a vital organ is prone to injury or tissue damage. In order to rectify physiological stress and physical damage to the skin, several antibiotics have been developed, commercialized and used frequently. The frequent use of antibiotics has caused the cells to develop resistance and use of high-dose drugs has resulted in side effects to other vital organs and systems. Therefore, there is an urgent need to develop a suitable platform to deliver bio-based drugs to the target tissue for regeneration using novel biomaterials, for slow and steady release of drugs with minimal or no side effects to other organs or systems. Accordingly, the CPMSN material was formulated and used in the present study. Also, *in vitro* and *in vivo* wound-healing properties of the formulated CPMSN biomaterial was determined. The delivery of CPMSN biomaterial in the wound regions of mice was found to downregulate pro-inflammatory cytokines. This could be the possible reason for conversion of
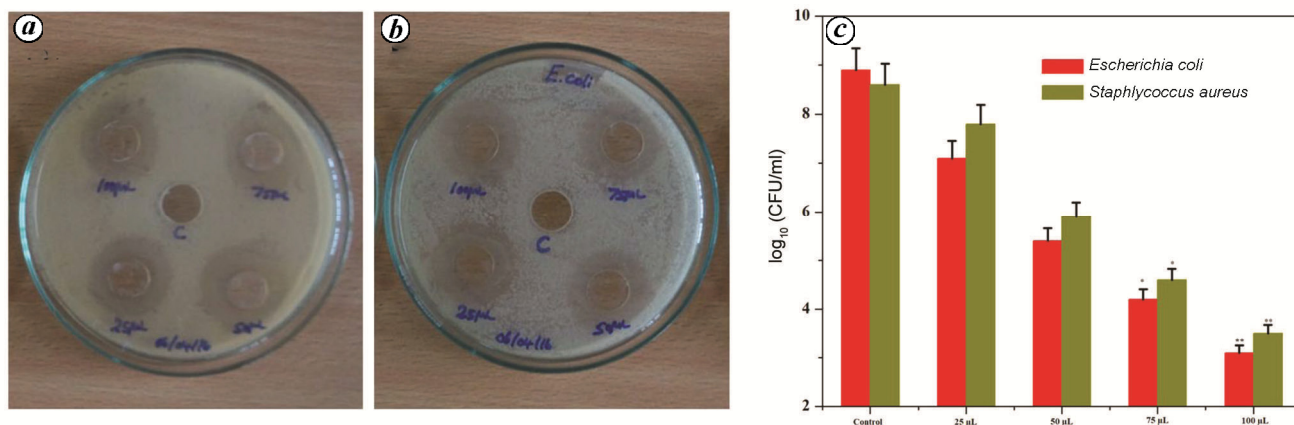
Figure 5. Dilution method to determine the minimal inhibitory concentration (MIC) of CPMSNs. Two bacterial strains. *a*, MRSA-*Staphylococcus aureus*. *b*, MDR-*Escherichia coli* were inoculated at 10^5 cells/ml on agar medium emulsified with various concentrations of CPMSN and distilled water used as control (0.05%). *c*, Estimation of bacterial colonies in control and CPMSNs-treated groups. Photographs were taken 24 h after inoculation for the CPMSN concentration (25, 50, 75 and 100 µl) tested.

M1 to M2 phase of macrophages that accounts for wound sealing[13]. However, the expression of several cytokines during wound healing is indispensible. In particular, TNF-α, IL-1 and TGF-β are known to overexpress during the wound-healing process. The present study highlights the significance of CPMSN biomaterial in the induction of immunological responses in favour of wound closure at different time intervals of treatment. The obtained results indicated that the mice model treated with CPMSN biomaterial stimulated re-epithelialization, wound contraction and fibroblast differentiation by decreasing inflammatory responses. Furthermore, the fabricated CPMSN biomaterial was found to have bacteria-killing efficacy that leads to overwhelming wound-healing activity. Our findings are in agreement with the reports of Rodero and Khosrotehrani[14], who well-documented the concept that wound healing is closely associated with physiological condition as well as immune response against bacterial pathogens at the wound sites.

In addition, TGF-β is playing a vital role in the granulation of tissues and accumulation of ECM proteins. Therefore, TGF-β level was estimated to ascertain its role in wound-healing enhancement following CPMSN treatment. The present finding showed that TGF-β levels were found to be high at day 21 in the CBMSN-treated group but returned to normal levels during treatment. At this juncture, the CPMSN was successfully incorporated into the wound areas as the CPMSN material is highly compatible with the natural tissue[15]. The results obtained in this study indicates that the incorporation of CPMSN into the wound areas significantly release the drugs namely TPT and QT, at low concentration. Hence, the formulated CPMSN serve as a wound-dressing material with high level of antimicrobial and wound healing properties. On the other hand, high levels of inflammation and wound infection can be attributed to the high levels of inflammatory and pro-inflammatory cytokines like TNF- and IL-4, which accounts for inhibition of bacterial growth at wounded sites[16].

In this study, TNF-levels in wounds were recorded to be lower in CPMSN-treated groups compared to control at day 21 post-wound. This might be due to the presence of TPT and QT that are known to have an inhibitory effect on the release of pro-inflammatory cytokines[17]. The CPMSN-treated group exhibited higher percentage of collagen, approximately 20% increase over control, within the wound ($P = 0.01$) on day 21, indicating good healing as collagen enhances wound strength and is crucial for processes involved in early stages of wound healing[18]. The findings of this study were consistent with earlier reports that demonstrated the presence of abundant collagen resulting in better wound healing. Macroscopic observations indicated that at 21 days post-wounding, re-epithelialization was more in CPMSN group than in the control. The ultimate aim of wound healing is fast recovery accompanied with minimum scar formation. The control of microbial infection of wound is also important for better healing and management. Post-operative wounds are usually infected by bacteria. Signs of bacterial infection of wounds are restlessness and scratching/biting of wound site. Other signs include delay in the onset of the proliferative and remodelling phases of the wound-healing process due to the release of free radicals and lytic enzymes at the wound site[19]. The delay in wound healing by these free radicals is achieved by their ability to destroy lipids, proteins and the extracellular matrix. This releases organic residues on the wounds to attract bacterial pathogens. Our results show that the designed CPMSN biomaterial destroys drug resistant bacterial pathogens[20].

The results showed that CPMSNs induced PMNs to increase/decrease amount of IL secretion. CPMSNs comprise of QT as an antioxidant, which has been reported to play a significant role in the wound-healing process by

protecting tissues from oxidative damage. It has been documented that CPMSNs with antibacterial and antioxidant properties enhance wound healing by accelerating wound contraction and re-epithelialization. They induce inflammatory cell migration and angiogenic activity favouring high vascularization of the neotissue[21]. Moreover, collagen type I and IV were synthesized under the granulation tissue and formation of the dermal–epidermal junction was observed. After 21 days, the new tissue was similar to native skin, especially with regard to its aesthetic aspect and its great flexibility. The presence of CPMSNs significantly delayed the appearance of macrophages and also reduced capillary ingrowth, fibroblast infiltration and mature collagen fibre deposition. These results indicated that the application of CPMSNs to skin improved the epithelial granular layer and increased granular density. Histological examination confirmed that the epithelialization rate had increased and deposition of collagen in the dermis was well organized as a result of covering the wounds with this nanomaterial. Furthermore, application of CPMSN to the skin resulted in lower production of TGF-β compared to the control. The results showed that CPMSN dressings provided effective absorption of exudates, ventilation for the wound, protection from infections and stimulation of the process of skin tissue regeneration[21,22].

Novel biological adhesives made from silica and polymeric derivatives were evaluated for their adhesive properties and biocompatibility[23,24]. Therefore, CS with acrylic groups was synthesized and cured by the addition of aqueous hydrogen peroxide solution as a radical initiator. This novel membrane favours fibroblast cell attachment and growth by providing a 3D environment, which mimics the ECM in skin and allows the cells to move through the fibrous structure. This results in interlayer growth throughout the membrane, thus favouring potential for deep and intricate wound-healing. At lower concentrations (<0.2 mg/ml), the polycationic CS on the CPMSN binds to the negatively charged bacterial surface to cause agglutination, while at higher concentrations, the larger number of positive charges imparts a net positive charge to the bacterial surfaces to keep them in suspension. The results of this study suggested that delayed wound healing was associated with an increased rate of systemic recurrence after creation of wound out. Reduced wound issues could be achieved due to the benefits of systemic recurrence rates and, ultimately death. In order to study the conflicting clamping and stimulating effects of CPMSN on normal wounds, bandages were removed from the wounds after 1 to 21 days of use. All application times resulted in a faster healing slope after removal compared to control wounds. A second soft and flexible layer allowed the material to follow the geometry of the wound and ensured good superficial contact. The results showed that CPMSN materials were well-tolerated and promoted good tissue regeneration. Therefore, the developed CPMSN biomaterial can be used as an agent for wound healing.

Conclusion

To the best of our knowledge, there are no previous reports on using combinatorial action of CS, QT and cRGD peptide with MSNs which help in wound-healing and are also antibacterial agents. The biodegradable CPMSN-displayed stumpy cytotoxicity, well-ordered degradability and high linkage strength in both *in vitro* and *in vivo* conditions[9]. The CPMSN comprising CS, QT and PAA accelerated wound healing and anti-bacterial activity. This biomaterial helped to improve adhesion strength, tunable degradability and showed promising results in *in vivo* wound-healing mice model. The CPMSN-related sticky biomaterial might provide a clinical option for wound closure by increase/decrease in some interleukin and cytokine responses to inflammation. As the CPMSN biomaterials is stable in a moist environment, it can help in the wound-healing process.

Disclosure: The authors declare no conflict of interest.

1. Volk, V. and Bohling, H., Comparative wound healing – are the small animal veterinarian's clinical patients an improved translational model for human wound healing research? *Wound Repair Regen.*, 2013, **21**(3), 372–381.
2. Gil, E., Panilaitis, B., Bellas, E. and Kaplan, D., Functionalized silk biomaterials for wound healing. *Adv. Healthcare Mater.*, 2013, **2**(1), 206–217.
3. Kamalathevan, P., Ooi, P. S. and Loo, Y. L., Silk-based biomaterials in cutaneous wound healing: a systematic review. *Adv. Skin Wound Care*, 2018, **31**(12), 565–573.
4. Klopfleisch, R. and Jung, F., The pathology of the foreign body reaction against biomaterials. *J. Biomed. Mater. Res. A*, 2017, **105**(3), 927–940.
5. Miller, E. *et al.*, Plasma-based biomaterials for the treatment of cutaneous radiation injury. *Wound Repair Regen.*, 2019, **27**(2), 139–149.
6. Nipun Babu, V. and Kannan, S., Enhanced delivery of baicalein using cinnamaldehyde cross-linked chitosan nanoparticle inducing apoptosis. *Int. J. Biol. Macromol.*, 2012, **51**, 1103–1108.
7. Vivek, R. *et al.*, HER2 targeted breast cancer therapy with switchable 'off/on' multifunctional 'smart' magnetic polymer core–shell nanocomposites. *ACS Appl. Mater. Interface.*, 2016, **8**, 2262–2279.
8. Kim, D., Mustoe, T. and Clark, R., Cutaneous wound healing in aging small mammals: a systematic review. *Wound Repair Regen.*, 2015, **23**(3), 318–339.
9. Murugan, C. *et al.*, Combinatorial nano carrier based drug delivery approach for amalgamation of anticancer agents in breast cancer cells: an improved nanomedicine strategy. *Sci. Rep.*, 2016, **6**, 34053.
10. Yin, G., Wang, Z., Wang, Z. and Wang, X., Topical application of quercetin improves wound healing in pressure ulcer lesions. *Exp. Dermatol.*, 2018, **27**(7), 779–786.
11. Sajadimajd, S. *et al.*, Advances on natural polyphenols as anticancer agents for skin cancer. *Pharmacol. Res.*, 2019; doi:10.1016/j.phrs.2019.104584.

12. Bradford, M. M., A rapid and sensitive method for the quantitation of microgram quantities of protein utilizing the principle of protein–dye binding. *Analyt. Biochem.*, 1976, **72**, 248–254.

13. Krzyszczyk, P., Schloss, R., Palmer, A. and Berthiaume, F., The role of macrophages in acute and chronic wound healing and interventions to promote pro-wound healing phenotypes. *Front. Physiol.*, 2018, **9**, 419–441.

14. Rodero, M. P. and Khosrotehrani, K., Skin wound healing modulation by macrophages. *Int. J. Clin. Exp. Pathol.*, 2010, **3**, 643–653.

15. Ju Yeh, C., Chuan Chen, C., Lii Leu, Y., Wei Lin, M., Miao Chiu, M. and Hu Cei Wang, S., The effects of artocarpin on wound healing: *in vitro* and *in vivo* studies. *Sci. Rep.*, 2017, **7**, 15599–15612.

16. Abarca-Buis, R. F. *et al.*, Mechanisms of epithelial thickening due to IL-1 signalling blockade and TNF-α administration differ during wound repair and regeneration. *Differentiation*, 2018, **99**, 10–20.

17. Delavary, B. M., van der Veer, W. M., Egmond, M. V., Niessen, F. B. and Beelen, R. H., Macrophages in skin injury and repair. *Immunobiology*, 2011, **216**, 753–762.

18. Zhao, P. *et al.*, Anti-aging pharmacology in cutaneous wound healing: effects of metformin, resveratrol, and rapamycin by local application. *Aging Cell*, 2017, **16**(5), 1083–1093.

19. Bian, W. *et al.*, OA-GL21, a novel bioactive peptide from *Odorrana andersonii*, accelerated the healing of skin wounds. *Biosci. Rep.*, 2018, **38**, 1–15.

20. Murugan, C., Venkatesan, S. and Kannan, S., Cancer therapeutic proficiency of dual – targeted mesoporous silica nanocomposite endorses combination drug delivery. *ACS Omega*, 2017, **2**, 7959–7975.

21. Nethi, S., Das, S., Ranjan Patra, C. and Mukherjee, S., Recent advances in inorganic nanomaterials for wound-healing applications. *Biomater. Sci.*, 2019, **7**, 2652–2674.

22. Quignard, S., Coradin, T., Powell, J. J. and Jugdaohsingh, R., Silica nanoaprticles as source of silicic acid favouring wound healing *in vitro*. *Colloids Surf. B*, 2017, **155**, 530–537.

23. Sundarraj, S., Thangam, R., Sujitha, M. V., Vimala, K. and Kannan, S., Ligand-conjugated mesoporous silica nanorattles based on enzyme targeted prodrug delivery system for effective lung cancer therapy. *Toxicol. Appl. Pharmacol.*, 2014, **275**, 232–243.

24. Vimala, K., Shanthi, K., Sundarraj, S. and Kannan, S., Synergistic effect of chemo-photothermal for breast cancer therapy using folic acid (FA) modified zinc oxide nanosheet. *J. Colloid Interface Sci.*, 2017, **488**, 92–108.